Real-time *in situ* Mueller matrix ellipsometry of GaSb nanopillars: observation of anisotropic local alignment

Ingar Stian Nerbø,[1,*] Sebastien Le Roy,[2] Martin Foldyna,[3] Elin Søndergård,[2] and Morten Kildemo[1]

[1]*Physics Department, Norwegian University of Science and Technology (NTNU) NO-7491 Norway*
[2]*UMR 125 Unit mixte CNRS/Saint-Gobain Laboratoire Surface du Verre et Interfaces 39 Quai Lucien Lefranc, F-93303 Aubervilliers, Cedex, France*
[3]*LPICM, Ecole polytechnique, CNRS, 91128 Palaiseau, France*

*ingar.nerbo@ntnu.no

Abstract: The formation of GaSb nanopillars by low energy ion sputtering is studied in real-time by spectroscopic Mueller matrix ellipsometry, from the initial formation in the smooth substrate until nanopillars with a height of 200 – 300 nm are formed. As the nanopillar height increased above 100 nm, coupling between orthogonal polarization modes was observed. *Ex situ* angle resolved Mueller polarimetry measurements revealed a 180° azimuth rotation symmetry in the off-diagonal Mueller elements, which can be explained by a biaxial material with different dielectric functions ε_x and ε_y in a plane parallel to the substrate. This polarization coupling can be caused by a tendency for local direction dependent alignment of the pillars, and such a tendency is confirmed by scanning electron microscopy. Such observations have not been made for GaSb nanopillars shorter than 100 nm, which have optical properties that can be modeled as a uniaxial effective medium.

© 2011 Optical Society of America

OCIS codes: (160.4236) Nanomaterials; (240.2130) Ellipsometry and polarimetry; (310.6628) Subwavelength structures, nanostructures.

References and links

1. I. S. Nerbø, S. Le Roy, M. Kildemo, and E. Søndergård, "Real-time in situ spectroscopic ellipsometry of gasb nanostructures during sputtering," Appl. Phys. Lett. **94**, 213105 (2009).
2. S. Le Roy, E. Søndergård, I. S. Nerbø, M. Kildemo, and M. Plapp, "Diffuse-interface model for nanopatterning induced by self-sustained ion-etch masking," Phys. Rev. B **81**, 161401 (2010).
3. S. Le Roy, E. Søndergård, I. S. Nerbø, and M. Kildemo, "In-situ and real time study of the formation of nanopatterns on gasb by ion abrasion," Phys. Rev. B (2011), in submission.
4. H. G. Tompkins and E. A. Irene, *Handbook of Ellipsometry* (William Andrew Publishing and Springer-Verlag GmbH and Co., 2005).
5. N. J. Podraza, C. Chen, I. An, G. M. Ferreira, P. I. Rovira, R. Messier, and R. W. Collins, "Analysis of the optical properties and structure of sculptured thin films from spectroscopic mueller matrix ellipsometry," Thin Solid Films **455-456**, 571–575 (2004).
6. G. Beydaghyan, C. Buzea, Y. Cui, C. Elliott, and K. Robbie, "Ex situ ellipsometric investigation of nanocolumns inclination angle of obliquely evaporated silicon thin films," Appl. Phys. Lett. **87**, 153103 (2005).

#145499 - $15.00 USD Received 6 Apr 2011; revised 1 Jun 2011; accepted 3 Jun 2011; published 14 Jun 2011

7. B. Gallas, N. Guth, J. Rivory, H. Arwin, R. Magnusson, G. Guida, J. Yang, and K. Robbie, "Nanostructured chiral silver thin films: a route to metamaterials at optical frequencies," Thin Solid Films, (2010), in production.
8. D. Schmidt, B. Booso, T. Hofmann, E. Schubert, A. Sarangan, and M. Schubert, "Generalized ellipsometry for monoclinic absorbing materials: determination of optical constants of Cr columnar thin films," Opt. Lett. **34**, 992 (2009).
9. I. S. Nerbø, S. Le Roy, M. Foldyna, M. Kildemo, and E. Søndergård, "Characterization of inclined GaSb nanopillars by Mueller matrix ellipsometry," J. Appl. Phys. **108**, 014307 (2010).
10. M. Ranjan, T. W. H. Oates, S. Facsko, and W. Möller, "Optical properties of silver nanowire arrays with 35 nm periodicity," Opt. Lett. **35**, 2576–2578 (2010).
11. D. Aspnes, J. Harbison, A. Studna, and L. Florez, "Reflectance-difference spectroscopy system for real-time measurements of crystal growth," Appl. Phys. Lett. **52**, 957–959 (1988).
12. J. Bremer and O. Hunderi, "Ras studies of laterally nanostructured surfaces," Phys. Stat. Solidi A **184**, 89–100 (2001).
13. W. Richter, "In-situ observation of movpe epitaxial growth," Appl. Phys. A **75**, 129–140 (2002).
14. F. Everts, H. Wormeester, and B. Poelsema, "Optical anisotropy induced by ion bombardment of Ag(001)," Phys. Rev. B **78**, 155419 (2008).
15. C. Chen, M. Horn, S. Pursel, C. Ross, and R. Collins, "The ultimate in real-time ellipsometry: multichannel mueller matrix spectroscopy," Appl. Surface Sci. **253**, 38–46 (2006).
16. E. Collett, *Polarized Light: Fundamentals and Applications* (Marcel Dekker, Inc., 2003).
17. P. Hauge, "Conventions and formulas for using the Mueller-Stokes calculus in ellipsometry," Surface Sci. **96**, 81–107 (1980).
18. D. W. Berreman, "Optics in stratified and anisotropic media: 4x4-matrix formulation," J. Opt. Soc. Am. **62**, 502–510 (1972).
19. M. Schubert, "Polarization-dependent optical parameters of arbitrarily anisotropic homogeneous layered systems," Phys. Rev. B **53**, 4265–4274 (1996).
20. A. De Martino, S. Ben Hatit, and M. Foldyna, "Mueller polarimetry in the back focal plane," in "Society of Photo-Optical Instrumentation Engineers (SPIE) Conference Series," (2007), vol. 6518.
21. B. H. Ibrahim, S. B. Hatit, and A. De Martino, "Angle resolved mueller polarimetry with a high numerical aperture and characterization of transparent biaxial samples," Appl. Opt. **48**, 5025–5034 (2009).
22. S. B. Hatit, M. Foldyna, A. De Martino, and B. Drévillon, "Angle-resolved mueller polarimeter using a microscope objective," Phys. Stat. Solidi A **205**, 743–747 (2008).
23. I. S. Nerbø , M. Kildemo, S. Le Roy, I. Simonsen, E. Søndergård, L. Holt, and J. Walmsley, "Characterisation of nanostructured GaSb : comparison between large-area optical and local direct microscopic techniques," Appl. Opt. **47**, 5130–5139 (2008).
24. T. Yamaguchi, S. Yoshida, and A. Kinbara, "Optical effect of the substrate on the anomalous absorption of aggregated silver films," Thin Solid Films **21**, 173–187 (1974).
25. E. Fort, C. Ricolleau, and J. Sau-Pueyo, "Dichroic thin films of silver nanoparticle chain arrays on facetted alumina templates," Nano Lett. **3**, 65–67 (2003).
26. S. Camelio, D. Babonneau, D. Lantiat, L. Simonot, and F. Pailloux, "Anisotropic optical properties of silver nanoparticle arrays on rippled dielectric surfaces produced by low-energy ion erosion," Phys. Rev. B **80**, 1–10 (2009).
27. C. Granqvist and O. Hunderi, "Optical properties of ultrafine gold particles," Phys. Rev. B **16**, 3513–3534 (1977).
28. S. Le Roy, E. Barthel, N. Brun, A. Lelarge, and E. Søndergård, "Self-sustained etch masking: a new concept to initiate the formation of nanopatterns during ion erosion," J. Appl. Phys. **106**, 094308 (2009).
29. J. E. Spanier and I. P. Herman, "Use of hybrid phenomenological and statistical effective-medium theories of dielectric functions to model the infrared reflectance of porous sic films," Phys. Rev. B **61**, 10437–10450 (2000).

1. Introduction

Spectroscopic ellipsometry (SE) has proved to be an efficient tool for real-time observation of the formation of nanostructured surfaces, *e.g.* the height evolution of GaSb nanopillars has been monitored during ion sputtering [1]. Real-time *in situ* measurements allow to follow the formation in time, and to find how the formation rate depends on experimental parameters, leading to a deeper understanding of the formation mechanisms of such structures [2, 3]. Such studies are not feasible with traditional *ex situ* microscopic characterization methods for nanoscale structures, such as atomic force microscopy (AFM) or scanning electron microscopy (SEM), due to time-demand and uncertainty of process parameters.

Ellipsometry is based on measuring the relative change of phase and amplitude between two orthogonal field components of reflected light. For reflections from an anisotropic material,

#145499 - $15.00 USD Received 6 Apr 2011; revised 1 Jun 2011; accepted 3 Jun 2011; published 14 Jun 2011
(C) 2011 OSA

there will in general be coupling between orthogonal field components. To fully characterize this coupling it is necessary to do generalized ellipsometry or Mueller matrix ellipsometry [4]. GaSb nanopillars prepared by sputtering with normal ion incidence, with a height less than 100 nm, have earlier been reported not to result in coupling between orthogonal polarization components, and to be modelled as a uniaxial effective material with the optic axis normal to the substrate [1]. How polarized light is affected by a reflection from such a surface can be completely characterized by standard ellipsometry. However, for larger nanopillars, the effective medium approximation is expected to fail as the size of the structure becomes comparable to the wavelength of light, and the uniaxial model will no longer be able to represent the optical properties of the pillars. In this study we report real-time *in situ* spectroscopic Mueller matrix measurements of GaSb during ion sputtering: from the initial formation in the smooth substrate, until pillars with heights of $200-300$ nm are formed. The Mueller matrix will contain information about possible anisotropic properties of the structure, caused by an anisotropic shape or organization of the pillars.

The anisotropic optical properties of a number of different nanostructures have previously been studied *ex situ* by generalized ellipsometry or Mueller matrix ellipsometry [5–10]. Reflectance-difference(anisotropy) spectroscopy (RDS/RAS) have been widely applied for real-time studies of surface anisotropies of semiconductors [11] and nanostructured surfaces [12–14]. RAS is highly sensitive, but can only measure the anisotropic part of the optical properties. In comparison Mueller matrix ellipsometry can measure the absolute dielectric function of an anisotropic material, not only the relative difference. Real-time Mueller matrix spectroscopy was demonstrated for the first time by Chen *et al.* [15], for characterization of geometrical optics scale roughness on ZnO. The reported roughness had isotropic optical properties, but its depolarizing properties made Mueller matrix measurements necessary. To our knowledge, generalized ellipsometry or Mueller matrix ellipsometry studies of an anisotropic nanostructured surface have not been performed in real-time before.

2. Theory and optical modeling

A Mueller matrix ellipsometer measures the 4×4 real valued Mueller matrix, which can describe any linear interaction of polarized light with a sample by transforming Stokes vectors representing the polarization state of light [16]. For non-depolarizing samples, the Mueller matrix can be used to overdetermine the normalized Jones matrix, containing the complex reflection coefficients [15]. The reflection coefficients (r_{ij}, with the subscripts i and j denoting the p and s directions) can be defined as

$$\begin{bmatrix} E_p \\ E_s \end{bmatrix}^{out} = \begin{bmatrix} r_{pp} & r_{ps} \\ r_{sp} & r_{ss} \end{bmatrix} \begin{bmatrix} E_p \\ E_s \end{bmatrix}^{inc},$$

with E_p and E_s denoting the complex field components parallel and orthogonal to the plane of incidence, respectively. The connection between the Jones and Mueller matrices for a non-depolarizing sample can be found in *e.g.* Ref. [17]. The Mueller matrix of a depolarizing sample has no equivalent Jones matrix. The reflection coefficients for a stack of homogeneous layers of optically anisotropic material can be calculated using Berreman's 4×4 differential matrix method [18, 19].

3. Experimental

A GaSb wafer (100) was sputtered for 10 minutes with 500 eV Ar^+ ions at normal incidence, with an ion flux of 0.32 mA/cm^2. *In situ* spectroscopic Mueller matrix measurements was performed every 5 seconds during sputtering, in the photon energy range of $1.5-2.8$ eV (MM16,

#145499 - $15.00 USD Received 6 Apr 2011; revised 1 Jun 2011; accepted 3 Jun 2011; published 14 Jun 2011
(C) 2011 OSA

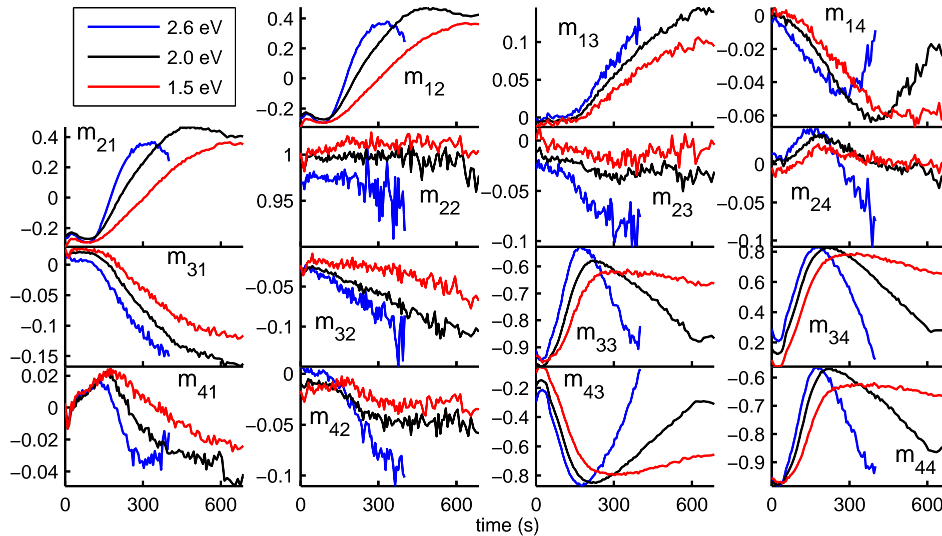

Fig. 1. Real-time Mueller matrix measurement of GaSb nanopillars, presented at three different photon energies. The 2.6 eV photon energy measurement is not presented for a sputtering time higher than 400 s, as after this time the surface becomes highly anti-reflective, and the optical signal becomes too low at high energies.

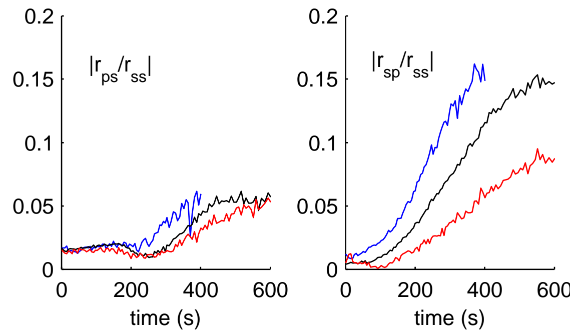

Fig. 2. Absolute values of the off-diagonal Jones elements, normalized by r_{ss}, derived from real-time Mueller matrix measurements of the formation of GaSb nanopillars, at photon energies of 2.6 eV (blue), 2.0 eV (black) and 1.5 eV (red).

Horiba Jobin Yvon), at an angle of incidence of 45°. The final nanostructured surface was studied *ex situ* by SEM. A sample prepared with identical sputtering conditions was also studied *ex situ* with a single wavelength (633 nm) angle resolved Mueller matrix polarimeter. The instrument applied a high numerical aperture (NA=0.95) microscope objective in a double pass configuration with its back focal plane imaged on a charge coupled device camera, allowing simultaneous measurements of reflected light at all azimuth angles and all angles of incidence below 62° [20–22].

4. Results and discussion

Figure 1 shows real-time *in situ* measurements of the Mueller matrix of the GaSb sample during sputtering, for three different photon energies. During the first $2-3$ minutes there is no

#145499 - $15.00 USD Received 6 Apr 2011; revised 1 Jun 2011; accepted 3 Jun 2011; published 14 Jun 2011
(C) 2011 OSA

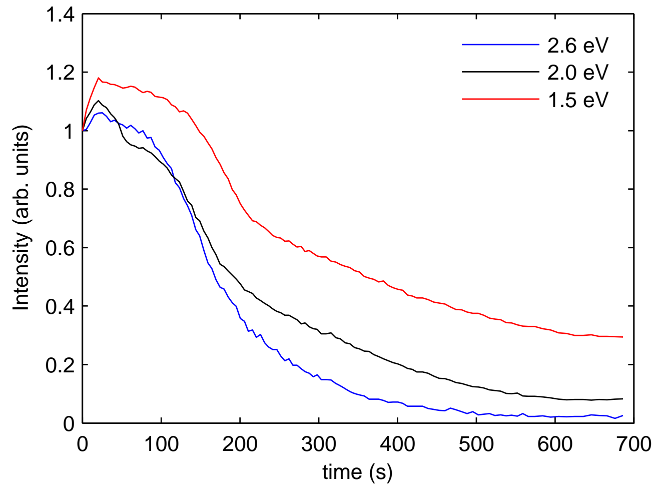

Fig. 3. Reflected intensity change from GaSb during sputtering, normalized by the reflected intensity before sputtering. The values are equal to the change in intensity refletance for unpolarized light (Mueller element M_{11}).

significant polarization coupling in the Mueller matrix, as all the four elements in the upper-right and lower-left corners are close to zero. After about 3 minutes of sputtering, polarization coupling becomes visible in the Mueller matrix and increases steadily until the end of the sputtering. To illustrate this more clearly, the absolute value of the normalized off-diagonal Jones elements, $|r_{ps}/r_{ss}|$ and $|r_{sp}/r_{ss}|$, have been derived from the Mueller matrix and are presented in Fig. 2. This polarization coupling indicate that the effective dielectric function is anisotropic in the plane parallel to the substrate, which is not consistent with a uniaxial material with the optic axis normal to the substrate. The reflected intensity change from the GaSb surface during sputtering is presented in Fig. 3. The nanopillars have a conical shape, which gives a gradient in the effective index of refraction [23], making the pillars anti-reflective. This means that the reflected light intensity decrease as the height of the pillars increase. After 400 s the curves for the 2.6 eV measurement have been cut in Figs. 1 and 2, as the noise level is too high.

The lateral anisotropy of the nanopillars could have several different causes. It was earlier reported that inclined GaSb pillars prepared by sputtering at oblique ion incidence has highly anisotropic optical properties [9], and such structures can be modeled as an effective uniaxial material with the optic axis parallel to the inclined pillar axis, resulting in polarization coupling in the Mueller matrix. A slight tilt (less than $1-2^{\circ}$) of the incident ion beam from the sample normal during the *in situ* measurements could cause the observed coupling. Another explanation could be that the pillars have an average laterally anisotropic shape, *e.g.* the pillars could have an elliptical instead of circular crossection. On the other hand, the pillars could individually have a uniaxial shape, but have an average anisotropic organization, *e.g.* a direction dependent nearest neighbor distance. Such a lateral anisotropy should result in the pillars having optical properties like a biaxial material.

To get a better understanding of the anisotropic optical properties of the sample, the final structure was studied by *ex situ* angle resolved Mueller matrix polarimetry. Fig. 4 presents a polar plot of the normalized Mueller elements m_{13} and m_{14}, where the radial coordinate represents the sine of the angle of incidence and the polar angle represents the azimuth sample orientation. These figures reveal important information about the symmetries of the structure. One can observe four lines in the polar plots where the Mueller elements are zero, correspond-

#145499 - $15.00 USD Received 6 Apr 2011; revised 1 Jun 2011; accepted 3 Jun 2011; published 14 Jun 2011
(C) 2011 OSA

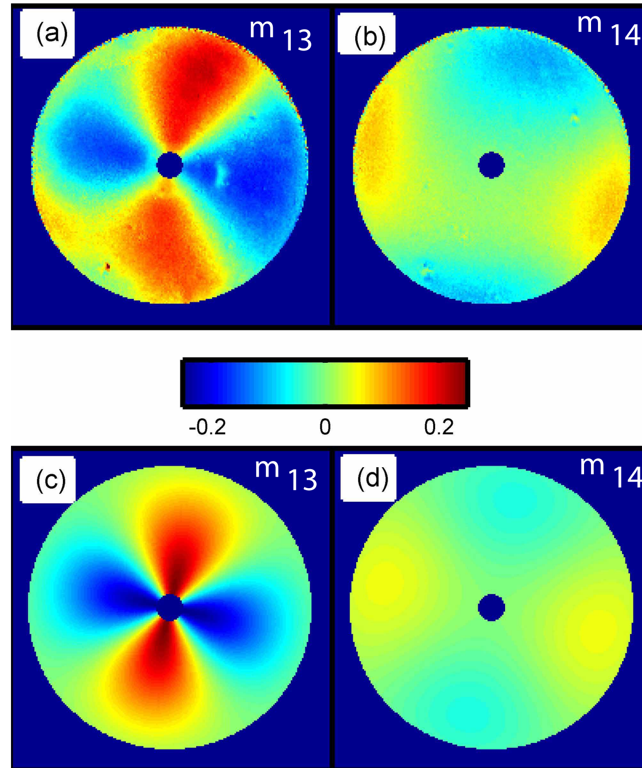

Fig. 4. Angle resolved Mueller matrix elements m_{13} (a) and m_{14} (b), and simulations of m_{13} (c) and m_{14} (d) for reflection from a biaxial effective medium. All at a wavelength of 633 nm. ($m_{13} = Re[r_{pp}r^{*}_{ps} + r_{sp}r^{*}_{ss}]/M_{11}$ and $m_{14} = Im[r_{pp}r^{*}_{ps} + r_{sp}r^{*}_{ss}]/M_{11}$).

ing to azimuth sample orientations separated by rotations of 90°, where there is no polarization coupling for all angles of incidence. The elements are also approximately symmetric for a rotation of 180°. These symmetries can be explained by the nanopillars behaving as a biaxially anisotropic material, with one of the intrinsic axes (referred to as the c-axis) normal to the substrate. The azimuth orientations resulting in no polarization coupling then correspond to the cases when one of the two other intrinsic axes lie in the plane of incidence. This symmetry implies that the polarization coupling observed in the real-time Mueller matrix measurements are mainly caused by a laterally anisotropic shape or organization. A small pillar inclination caused by slightly oblique ion incidence, would instead give only two azimuth orientations with no polarization coupling (with the pillars inclined in the plane of incidence), and a change of sign of element m_{13} and m_{14} for an azimuth rotation of 180°. A small tilt however, could still cause the slight difference between the left and right lobe of Fig. 4(a).

To study the shape and size of the final structure, SEM images of the samples were taken *ex situ* after sputtering. A crossection image of the surface is presented in Fig. 5(b), where pillars with a height of $250-300$ nm can be seen. Figure 5(c) shows an overview of the surface, where apparently randomly distributed pillars can be seen. The power spectral density (PSD) of the

#145499 - $15.00 USD Received 6 Apr 2011; revised 1 Jun 2011; accepted 3 Jun 2011; published 14 Jun 2011
(C) 2011 OSA

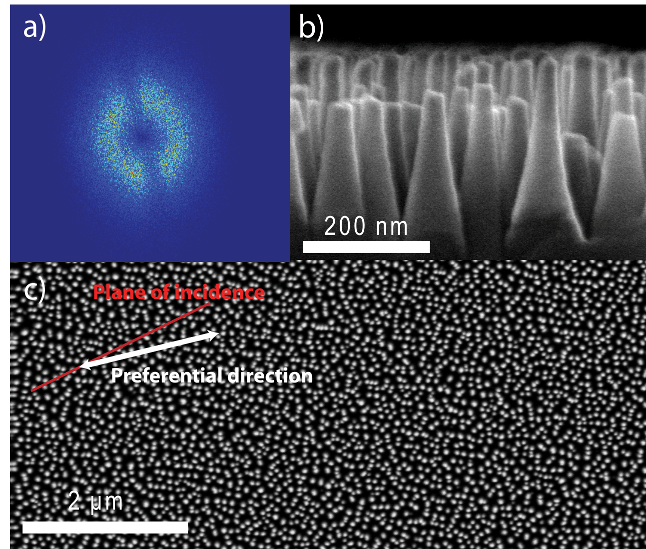

Fig. 5. (a) Power spectral density of the normal view SEM image (magnified), (b) GaSb pillars made by normal incidence sputtering, crosssection SEM image, and (c) normal view SEM image. The direction corresponding to the line in the power spectral density is denoted by the white arrow, together with the plane of incidence of the *in situ* Mueller matrix measurements.

SEM image (Fig. 5(a)) shows signs of an anisotropic organization, breaking the symmetry in the lateral plane. Randomly distributed circular structures corresponds to a donut shape in the PSD. The observed oppositely placed holes in the donut indicate a longer nearest neighbor distance in this direction (the opposite of alignment). From the SEM image one can see some tendency of local alignment of neighboring pillars along apparently random directions (lines of $4-10$ pillars are observed). The PSD indicate that local alignment is less likely in the direction corresponding to the holes in the donut shape. This direction is marked in the normal view SEM image in Fig. 5(c), and was found to be rotated by an angle of 13° from the plane of incidence of the *in situ* ellipsometry measurements.

In the first 3 minutes of sputtering, the measured Mueller matrix is approximately block-diagonal, and the height evolution of the pillars can be found by fitting the previously reported graded uniaxial effective medium model [1] to the non-zero Muller elements. In this model the pillars are treated as a stack of cylinders with decreasing diameter. Each cylinder define a layer, with an effective dielectric function found by a generalized anisotropic Bruggeman effective medium equation (see the Appendix). The heights of the GaSb nanopillars derived from this model are presented in Fig. 6, together with the χ^2 error function (calculated for an assumed experimental uncertainty of $\sigma = 0.01$ in the measured Mueller elements). After a short initial period of 30 s, the pillars start to form with a steady height increase of about 1nm a second. After 3 minutes of sputtering, the pillars have reached a height of about 120 nm, and the error function χ^2 starts to increase rapidly. This is about the same time as the polarization coupling becomes visible in the measured Mueller matrix, and the uniaxial effective medium model can no longer be applied. In addition, the reduced reflectivity of the pillars leads to a higher noise level at high energies, which also contributes to the increase in χ^2.

The observed lateral anisotropy (polarization coupling) was ascribed to the effective optical properties of the nanopillars being biaxially anisotropic, with one of the intrinsic axes normal

#145499 - $15.00 USD Received 6 Apr 2011; revised 1 Jun 2011; accepted 3 Jun 2011; published 14 Jun 2011
(C) 2011 OSA

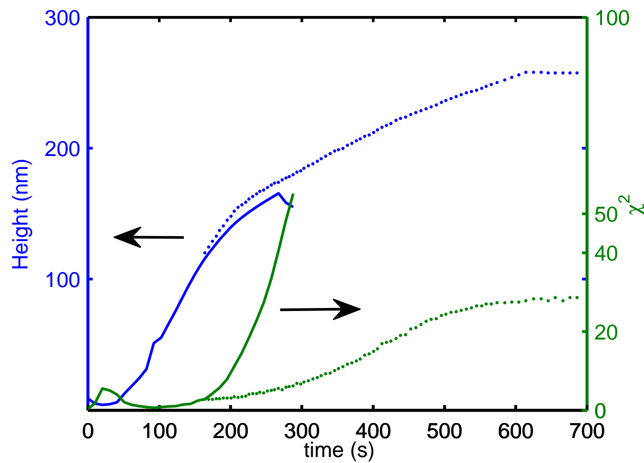

Fig. 6. Thickness of an graded anisotropic effective medium layer fitted to *in situ* Mueller matrix measurements of GaSb during sputtering, together with the error function χ^2. In the beginning a uniaxial model was applied (solid line), after 3 minutes a biaxial model (dots) was found to better represent the pillars.

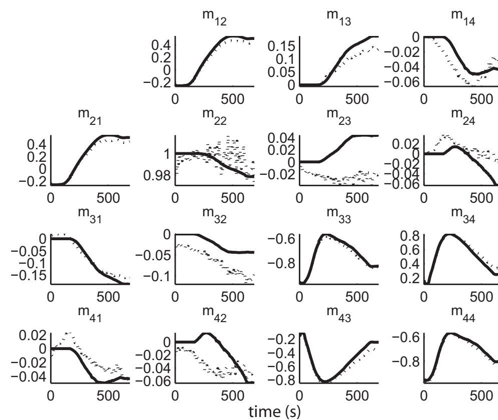

Fig. 7. Fitted Mueller matrix (solid) and experimental measurements (dots) at 2.0 eV.

#145499 - $15.00 USD Received 6 Apr 2011; revised 1 Jun 2011; accepted 3 Jun 2011; published 14 Jun 2011

(C) 2011 OSA

to the substrate. From SEM images this was concluded to be caused an average anisotropic organization. This can not be treated by the anisotropic Bruggeman equation (Eq. (1) in the Appendix), which is independent of the spatial organization. Extended effective medium models including neighbor interactions have been discussed in the literature by *e.g.* Yamaguchi *et. al* [24], and an extended Maxwell-Garnett equation has been applied to include anisotropic neighbor interactions in metallic nanostrucures [25, 26]. Such a model needs detailed information about the local ordering of the structures, taken from *e.g.* SEM-images. This information is not available for the *in situ* measurements of the formation of the GaSb nanopillars. A possible anisotropic ordering is instead crudely approximated by letting the depolarization factors L_a and L_b represent an "effective" shape, *i.e.* an anisotropic ordering is modeled by letting the pillars have an effective elliptical crossection. The use of effective depolarization factors to model neighbor interactions was introduced by Granqvist and Hunderi [27]. Figure 4(c) and 4(d) shows simulations of angle resolved Mueller elements m_{13} and m_{14} for such a biaxial model, which fits qualitatively well with the experimental measurements. The effective depolarization factors $L_a = 0.47$, $L_b = 0.53$ and $L_c = 0$ were used along the three principal axes, with the c-axis pointing normal to the substrate. A pillar height of 290 nm and top and bottom relative diameter of $D_2 = 0.1$ and $D_1 = 1$ (filling factor calculated for dense hexagonal ordering) was used in the simulation (see Appendix).

Fits of a biaxial model to the real-time measurements of the pillar formation after 3 minutes of sputtering are presented in Fig. 7, with the resulting pillar height and χ^2 values shown in Fig. 6. From the the measurement of the final structure, an effective depolarization factor of $L_a = 0.54$ was found for one of the principal axes in the lateral plane, rotated by an angle of 12° from the plane of incidence. The other principal axis in the lateral plane was set to have $L_b = 1 - L_a$, and the the depolarization factor for the last axis along the surface normal was set to $L_c = 0$. The orientation of the *a*-axis corresponds well with the direction corresponding to the holes in the donut shaped PSD in Fig. 5(a). As one would expect, the effective depolarization factor is highest along the direction with less local alignment. For the remaining real-time measurements, the orientation of the principal axes of the effective medium was fixed to be the same as the one found for the final measurement. This is reasonable as the angle was confirmed by SEM, and as the azimuth rotation of the principal axes are expected to be coupled to the depolarization factors for fits at ellipsometry measurements at a single azimuth sample orientation. The fit was limited to the photon energy range of $1.5 - 2.0$ eV due to the increased noise level caused by the reduced reflectivity from high pillars. In Fig. 6, a great improvement of χ^2 is observed for the biaxial model compared to the uniaxial model. Still, an increase in χ^2 with time is observed also for the more complex biaxial model, which is as expected since effective medium should not be valid for structures with a size comparable to the wavelength of light. The pillar height need not be the critical parameter for failure of the effective medium model, as interference effects normal to the substrate are included in the transfer matrix calculations for the reflection coefficients. More important is the lateral size, which must be sufficiently small for the model to be valid. The evolution of this size can however not be observed from the Mueller matrix measurements. Earlier reports from *ex situ* AFM studies on GaSb sputtered with different ion energies found that the lateral size of the pillars increase with energy [3]. For pillars sputtered with an ion energy of 300 and 400 eV, the lateral size was found to saturate to a constant value early in the formation. For samples sputtered with an ion energy of 500 eV, the lateral size of the pillars was found to increase for the first 5 minutes of sputtering. This means that the lateral size is increasing in the range where the χ^2 value is increasing. The fitted height seems, however, to give a reasonable approximation to the pillar height, with a final value of 250 nm which correspond well to the pillar height of 250-300 nm as observed in the SEM image. The resulting height evolution during sputtering is also equal to the observation

#145499 - $15.00 USD Received 6 Apr 2011; revised 1 Jun 2011; accepted 3 Jun 2011; published 14 Jun 2011
(C) 2011 OSA

of sputtering at lower energy [1], with a transition to a slower formation rate, but no saturation. This indicates that the formation mechanism reported in Ref. [2] is also valid for the formation of large pillars formed by sputtering at the higher ion energy of 500 eV.

The origin of the anisotropic ordering in the lateral dimension is not fully understood. As the formation does not depend on the crystal orientation of the substrate [28], there should not be any preferential direction for sputtering at normal ion incident. However, this symmetry could be broken by a small deviation of the ion incidence from the surface normal. Another explanation could be an initial anisotropic substrate roughness from the wafer polishing.

5. Conclusion

The formation of GaSb nanopillars by sputtering with 500 eV Ar^+ ions has been monitored in real-time by Mueller matrix ellipsometry. For the first 3 minutes the optical properties of the nanopillars were modeled by a graded uniaxial effective medium model. After 3 minutes, as the pillar height surpassed 100 nm, coupling between orthogonal polarization modes was observed from the measurements. From *ex situ* angle resolved Mueller matrix polarimetry of the final structure, this coupling was attributed to the pillars having effective biaxial optical properties, with one intrinsic axis normal to the substrate. Fourier analysis of a scanning electron microscope image of the final nanopillars, shows that the lateral anisotropy can be attributed to a direction dependent nearest neighbor distance. Each individual pillar has a uniaxial symmetry, the biaxial symmetry comes from the anisotropic organization of the pillars.

6. Appendix

It was earlier reported [1] that GaSb nanopillars with a height less than 100 nm could be modeled as a graded uniaxial effective medium, by treating the pillars as a stack of cylinders with decreasing diameter. Each cylinder in the stack constitute an effective layer with an effective dielectric tensor found by using a generalized Bruggeman effective medium equation for ellipsoidal inclusions [29]

$$f_{GaSb}\frac{\varepsilon_{GaSb}-\varepsilon_{ii}}{\varepsilon_{ii}+L_i(\varepsilon_{GaSb}-\varepsilon_{ii})}+f_v\frac{\varepsilon_v-\varepsilon_{ii}}{\varepsilon_{ii}+L_i(\varepsilon_v-\varepsilon_{ii})}=0, \tag{1}$$

where f and ε denote the filling factors and complex dielectric functions, respectively, with the subscript *GaSb* referring to the crystalline core, and v to the surrounding void. L_i denotes the depolarization factor in direction i (along a principal axis of the structure) and ε_{ii} is the effective dielectric function in direction i. For cylindrical inclusions $L_{||}=0.5$ (parallel to the mean surface) and $L_{\perp}=0$ (perpendicular to the mean surface). This gives a uniaxial anisotropic material with the optic axis normal to the mean surface, resulting in no coupling between orthogonal field components for reflected light ($r_{ps}=r_{sp}=0$). If the cylinder cross-sections are elliptical instead of circular, and all have the same orientation, the depolarization factors will be different along the minor and major axis ($L_x \neq L_y$), giving a biaxial anisotropic material, which in general lead to $r_{ps}\neq 0$ and $r_{sp}\neq 0$. The uniaxial symmetry can also be broken by an anisotropic ordering, *e.g.* by a different pillar separation along different directions. This can not be treated by Eq. (1), which is independent on spatial organization.

On average the GaSb pillars have 6 nearest neighbors [23], hence the filling factors have been calculated for a hexagonal lattice,

$$f_{GaSb}(n)=\frac{\pi}{\sqrt{12}}d^2(n),$$

where $d(n)$ is the diameter of the cylinder of layer n, which varies linearly from the bottom diameter D_1 to the top diameter D_2. The bottom and top diameters D_1 and D_2 are normalized

#145499 - $15.00 USD Received 6 Apr 2011; revised 1 Jun 2011; accepted 3 Jun 2011; published 14 Jun 2011
(C) 2011 OSA

to the nearest neighbor distance, since only the volume filling factors influence the effective medium. This means that the lateral size of the pillars can not be found from ellipsometry measurements when the effective medium approximation is valid.

#145499 - $15.00 USD Received 6 Apr 2011; revised 1 Jun 2011; accepted 3 Jun 2011; published 14 Jun 2011
(C) 2011 OSA